Some Wind and Instability Parameters Associated With Strong and Violent Tornadoes 1. Wind Shear and Helicity

JONATHAN M. DAVIES

Pratt, Kansas 67124

ROBERT H. JOHNS

National Severe Storms Forecast Center, Kansas City, Missouri 64106

1. INTRODUCTION

Although the vertical wind profile through the troposphere has been recognized to be important in tornado development since the beginning of tornado forecasting efforts in the 1950s, only recently have researchers begun to investigate more detailed characteristics of wind profiles contributing to low-level mesocyclone formation and tornado production in supercell thunderstorms. *Davies-Jones et al.* [1990] provide an overview of recent work completed in this area. From modeling results and storm observations, it appears that both (1) the wind profile in the low levels (i.e., the storm inflow layer) and (2) the strength of the wind field and shear extending through a deeper layer of the troposphere (i.e., through middle levels) are important to supercell-induced tornado development.

Regarding the low-level wind profile, mean shear [*Rasmussen and Wilhelmson*, 1983; *Davies*, 1989] is one parameter that has been used for assessing the veering of winds with height and turning of the hodograph associated with supercell thunderstorms. More recently, storm-relative helicity [*Lilly*, 1986; *Davies-Jones et al.*, 1990], which addresses the importance of the wind fields viewed from a storm's frame of reference, has become recognized as an effective parameter for measuring rotational potential in the low-level wind field. Helicity in the storm inflow layer is associated with streamwise vorticity [*Davies-Jones*, 1984] which, when "ingested" and tilted into the storm updraft, induces rotation. Also, numerical simulations by *Brooks and Wilhelmson* [1990], *Brooks et al.* [1992], and *McCaul* [1990] demonstrate the development of a mesolow in the inflow region of tornadic supercells, initiated by the dynamical interaction of the updraft with shear-induced vertical pressure forces [*Rotunno and Klemp*, 1982] that are largely a result of low-level curvature shear and helicity. This feature serves to intensify the vertical velocity of the growing updraft, as well as to strengthen inflow into the storm, an important requirement noted by *Lazarus and Droegemeier* [1990].

The strength of the wind fields and shear through a layer deeper than the low levels is also significant in supercell development. While low-level curvature shear is an important factor for producing the vertical pressure gradient mentioned in the prior paragraph, *Weisman and Klemp* [1986] note that it is also necessary for the vertical wind shear to extend through middle levels of the troposphere to sustain a rotating updraft via shear-induced pressure forces. One measure of this deeper ambient shear is the U parameter in the denominator of the Bulk Richardson Number [*Weisman and Klemp*, 1982, 1986]. *Doswell* [1991] also notes that middle-level winds of sufficient strength are a necessary component of hodographs that can support supercell development. A similar requirement is mentioned by *McCaul* [1991], who notes that 700 mbar wind speeds show good correlation with tropical cyclone tornado outbreaks. Strong middle-level winds may move precipitation downwind out of the upper portion of the updraft (or in some cases tilt the updraft so that precipitation falls out downwind), thereby eliminating a potential impediment to the development of a strong and sustained updraft.

On the basis of the above discussion, the following wind parameters were chosen for examination in this paper: (1) low-level mean shear (0–2 km/0–3 km/0–4 km above ground

The Tornado: Its Structure, Dynamics, Prediction, and Hazards.
Geophysical Monograph 79

level (AGL)), (2) storm-relative low-level helicity (0–2 km/0–3 km/0–4 km AGL), (3) Bulk Richardson Number shear (U) (boundary layer through 6 km AGL), and (4) mean wind speed in the middle levels (3–6 km AGL). *Johns et al.* [1990] (henceforth referred to as JDL) assembled a large and comprehensive data set of strong and violent mesocyclone-induced tornadoes (242 cases) for the purpose of examining the associated mean shear and buoyancy values. The same data set is utilized in this study to examine the aforementioned wind parameters, with suggestions for possible application to operational forecasting.

2. Case Selection Methodology

As described by JDL, Storm Data was examined systematically for the 10-year period April 1980 through March 1990. All nonlocalized tornado outbreaks that involved six or more tornadoes were selected, with the added requirement that two or more of the tornadoes be F2 or greater in intensity and separated by at least 60 nautical miles (111 km). Also, any F3 or greater intensity tornado accompanied by an uncontaminated proximity sounding was selected. These criteria were used in an attempt to eliminate most tornadoes of nonsupercell origin [*Wakimoto and Wilson*, 1989]. In large outbreaks, more than one case was selected if the constituent tornadoes were separated by ≥200 nautical miles (370 km) in distance or ≥10 hours in time.

3. Determination of Parameter Values

As discussed in detail by JDL, parameters computed from rawinsonde observations were either used directly or interpolated, depending on tornado case time and distance relative to soundings. In general, if a tornado case occurred within 3 hours and 75 statute miles (121 km) of an uncontaminated sounding in the warm sector, parameters computed from the observation were used directly. If the tornado case was more removed in distance, yet within 3 hours of sounding time, an interpolation was performed between parameter values from two or more soundings, depending on the availability and location of adjacent warm sector rawinsonde observations. If the tornado case was more removed in time, an interpolation of sounding parameter values in time and distance was performed by observing the evolution of wind features between sounding times, provided that wind fields were well defined on the synoptic scale. Cases that did not meet these criteria or that involved significant amounts of missing data were not accepted into the data set.

The limitations of the coarse rawinsonde network are well known. In an attempt to incorporate localized data, surface wind observations were also examined for each case. If the wind direction from a surface observation nearby in the warm sector exhibited significant backing (i.e., ≥20°) when compared to the surface wind of the sounding(s) associated with the case, the wind from the surface observation was blended into the sounding wind profile(s) for computing parameter values such as helicity and mean low-level shear. In spite of this effort to incorporate local data, the authors recognize that mesoscale variations not detected by the sounding network or surface observations can have major impact on thunderstorm behavior. Therefore parameter values obtained in this study can be viewed as only roughly representative of the actual prestorm wind environments for each case. By limiting the study to cases from nonlocalized tornado outbreaks, the probability is increased that rawinsonde network observations sampled at least some aspects of the wind environments supporting the observed tornadic supercell thunderstorms.

4. Mean Shear Results

From *Rasmussen and Wilhelmson* [1983], mean shear (S) is essentially

$$S = \text{hodograph length (m s}^{-1}\text{)/depth of layer (m)}$$

"Positive" mean shear [*Davies*, 1989], as amended by JDL, modifies this definition by setting the shear magnitude to zero for those hodograph segments where the ground-relative winds back significantly with height. Unlike storm-relative helicity, mean shear does not consider storm motion and is computationally very sensitive to the fine-scale wind structure. Recognizing these limitations, positive mean shear can, in many cases, provide an estimated assessment of rotational potential when a storm motion is not available.

Average positive mean shear magnitudes ($\times 10^{-3}$ s^{-1}) were computed for the 242 cases in the JDL data set using three atmospheric depths (AGL) for comparison:

0- 2-km average positive shear	13.6
0- 3-km average positive shear	10.7
0- 4-km average positive shear	9.1

The fact that the 0- 2-km average positive shear is larger than both the 0- 3-km and 0- 4-km averages suggests that in most cases a majority of the low-level wind shear is below 2 km AGL, similar to results from *Davies* [1989] using a smaller data set.

Grouping cases by tornado intensity (205 strong and 37 violent tornado cases), average positive mean shear values were

	Strong(F2/F3)	Violent(F4/F5)
0- 2-km average positive shear	13.4	14.7
0- 3-km average positive shear	10.5	11.7
0- 4-km average positive shear	9.0	10.0

These values suggest that, on an average, violent tornadoes occur with higher values of low-level positive mean wind shear than do tornadoes of lesser intensity.

5. Estimation of Storm Motion for Storm-Relative Helicity Computations

In order to calculate storm-relative helicity a storm motion is required. Storm motions originally were not obtained for

the JDL data set. For this study the authors have examined a subset of cases for which radar imagery was available at the National Severe Storms Forecast Center. This subset of 31 cases contains tornadoes that occurred during the period 1988–1990. Two of the cases from 1990 were not in the original JDL data set. Mean environmental winds (0- 6-km AGL [after *Weisman and Klemp*, 1986]) were computed from the sounding data for these cases, and comparisons were made with the storm motions obtained from the radar data. Though the storm motion sample is small, the cases appear to represent all seasons and most areas of the country east of the Rocky Mountains. It should be noted that the storm motion deviations here are not exactly comparable to *Maddox* [1976], *Darkow and McCann* [1977], and *Bluestein and Parks* [1983], who computed the mean wind through much deeper layers that generally encompassed the troposphere.

5.1. *Observed Storm Motions From the Data Subset*

The directional deviations within the 31 case subset vary from 2° left to 42° right of the 0- 6-km mean wind. Speed deviations vary from 58 to 158% of the 0- 6-km mean wind speed. It is notable that five of the cases moved faster than the mean wind speed; four of these were associated with bow echo structures [see *Doswell et al.*, 1990]. From these results it is apparent that for any given sample of tornado-producing supercell storms there can be a wide range of deviant motions when compared to the 0- 6-km mean environmental wind. This fact illustrates that without a better understanding of the complex problem of storm motion it will be difficult to implement a predictive cell movement procedure that will be successful in all cases.

Despite this problem a closer examination of the storm motion subset reveals some useful general information. Mean deviant storm motion for the 31 cases is 20° right of the 0- 6-km mean wind at 89% of the mean wind speed (or 20R89, as deviations will henceforth be annotated). Roughly half of the subset (15 cases) exhibits a directional deviation within 5° of this mean. This suggests that when considering supercell development, a motion deviation assumption of 20R85 or 20R90 would be a reasonably accurate forecast motion estimate roughly 50% of the time.

Some storm motion differences are apparent when grouping cases by both season and geographical locale. From the data subset, tornadic storms in the Great Plains during March through June (eight cases) display a mean motion of 27R80, while tornadic storms east of the Mississippi during November through February (11 cases) exhibit a mean motion of 18R97. The Great Plains storms have a directional deviation spread ranging from 13° to 37° right of the mean wind (with only one of eight cases less than 20° right) and a speed deviation spread ranging from 61 to 122% of the mean wind (only one case exceeded 100% of the mean wind speed). In contrast, the cool season storms east of the Mississippi have a smaller directional deviation spread, ranging from 12° to 24° right of the mean wind (six of 11 cases moved less than 20° right) and a speed deviation spread ranging from 77 to 122% (three of 11 cases moved at 100% or more of the mean wind speed). This difference suggests that the strength of the wind fields (which varies by season and locale) may play a significant part in storm motion.

5.2. *Storm Motion Related to Wind Field Strength*

In the 31 case subset, extreme right-moving storms (i.e., >25° right) are found to be associated with significantly weaker wind fields (0- 6-km mean wind speeds averaging 32 knots (16.5 m s^{-1})) than the other cases (0- 6-km mean wind speeds averaging 46 knots (23.7 m s^{-1})). This tendency for tornadic storms in relatively weak wind fields (i.e., 0- 6-km mean wind magnitudes <30–35 knots (15.5–18.0 m s^{-1})) to deviate increasingly right of the mean wind also can be seen in a study by *Darkow and McCann* [1977]. If their Figures 3*a* and 1*a* are compared, it becomes apparent that their extreme right-moving storms occurred in significantly weaker wind fields when compared to their data set as a whole.

The weakest 0- 6-km mean wind speeds found in the 31 case subset were near 20 knots (10.3 m s^{-1}), suggesting that mean wind speeds of lesser magnitude may be too weak to support strong or violent tornadoes in supercell thunderstorms. For purposes of this discussion, relatively "weak" wind fields that can support significant supercell-induced tornadoes will be defined as those with 0- 6-km mean wind speeds ≤30 knots (15.5 m s^{-1}) and ≥20 knots (10.3 m s^{1}).

5.3. *Suggested Storm Motion Assumptions*

On the basis of the above discussion, some rough first guess assumptions can be suggested regarding storm movement for right-moving cells in a given wind regime that is potentially tornadic. For environments characterized by relatively strong wind fields (i.e., 0- 6-km mean wind speeds >30 kt) a reasonable first guess movement would be a motion such as 20R85, similar to the 31-case subset mean deviant motion of 20R89. The storms in the subset that are not extreme right movers yield a mean deviant motion of 16R86, also close to 20R85. When weaker wind fields are involved (i.e., 0- 6-km mean wind speeds ≤30 knots (15.5 m s^{1})), a motion closer to 30R75, as used by *Maddox* [1976], is probably more appropriate. This is suggested by the fact that the storms in the 31-case subset that were extreme right movers traveling at less than the mean wind speed yielded a mean deviant motion of 34R76, close to a 30R75 assumption. It should be strongly emphasized that these estimates are only general reference points and do not address many other factors that affect storm motion, such as the orientation of boundaries and low-level forcing.

For this study, these rough assumptions will provide starting points, in lieu of actual observed storm motions, for examination of storm-relative helicity utilizing the JDL data set.

6. Storm-Relative Helicity Results

For this study, the authors have computed integrated total storm-relative helicity (H) for specific layers. The computation used is that of *Davies-Jones et al.* [1990]:

$H = -2 \times$ the signed area swept out by the storm-relative wind vector while ascending through a layer

Units are $m^2\ s^{-2}$ (identical to J kg^{-1}). Helicity is useful in measuring rotational potential because it has a sound physical link to overall updraft rotation and is sensitive to storm motion while remaining computationally insensitive to the fine-scale wind structure.

First, observed helicity values obtained from the 31-case storm motion subset will be examined. Then, utilizing the storm motion refinement assumptions from section 5, helicity values will be examined using the entire 242-case JDL data set.

6.1. *Observed Helicity From the Storm Motion Subset*

Helicity magnitudes were computed for the observed storm motions of the 31 subset cases and the same atmospheric layers (AGL) used previously in computing mean shear. Mean helicity magnitudes ($m^2\ s^{-2}$) for the three layers were as follows.

0- 2-km mean observed helicity	392
0- 3-km mean observed helicity	416
0- 4-km mean observed helicity	428

Note that most of the low-level helicity resides below 2 km AGL, similar to the mean shear results in section 4. An average of 94% of the 0- 3-km helicity is located within the 0- 2-km layer, and an average of 92% of the 0- 4-km helicity is located within the 0- 2-km layer.

The 31 cases (21 strong and 10 violent tornado cases) were also examined from the standpoint of helicity and tornado intensity:

	Strong(F2/F3)	Violent(F4/F5)
0- 2-km mean observed helicity	359	460
0- 3-km mean observed helicity	369	519
0- 4-km mean observed helicity	378	539

Results suggest that violent tornadoes, on an average, occur with larger helicity magnitudes than do strong tornadoes. This agrees with the general helicity guidelines presented by *Davies-Jones et al.* [1990] for strong and violent tornado development.

6.2. *Helicity Using the JDL Data Set and an Assumed Storm Motion*

For computing helicity, storm motions were estimated by applying a 20R85 assumption when 0- 6-km mean wind speeds were >30 knots (15 m s^{-1}), and a 30R75 assumption when 0- 6-km mean wind speeds were ≤30 knots (15 m s^{-1}) (see section 5). Helicity magnitudes were computed for the same three lower tropospheric layers examined using the 31 case storm motion subset, yielding the following mean values for the 242 cases.

0- 2-km mean assumed helicity	332
0- 3-km mean assumed helicity	356
0- 4-km mean assumed helicity	375

As with the 31-case subset, it is notable that so much of the low-level helicity is below 2 km AGL.

Grouping cases by tornado intensity (205 strong and 37 violent tornado cases), helicity values were computed using the same motion assumptions:

	Strong(F2/F3)	Violent(F4/F5)
0- 2-km mean assumed helicity	317	415
0- 3-km mean assumed helicity	339	452
0- 4-km mean assumed helicity	357	478

As with observed helicity from the 31 case subset, the larger data set yields similar results, showing violent tornadoes occur, on an average, in environments with larger helicity values than do strong tornadoes. However, notable exceptions certainly do occur, as will be seen in section 10.

For the 29 overlapping cases between the storm motion subset and the JDL data set, over half the mean helicity values computed using the motion assumptions were within 15% of the observed values, and all but eight cases were within 20% of the observed value. It therefore appears that the 20R85/30R75 assumptions based on general strength of the wind fields are useful starting points for generating helicity output.

Using this approach, Figure 1 illustrates a helicity forecast derived from the National Meteorological Center's Limited Fine Mesh (LFM) model, blending winds aloft forecast data with surface winds from Model Output Statistics (MOS) forecast guidance. For each output station the 0- 6-km mean wind direction and speed are printed along with helicity values computed using storm motion deviations of 20R85 and 30R75 relative to the 0- 6-km mean wind. This would allow a forecaster to see how the helicity changes with increasing storm deviation to the right at different locations plotted on the same map. On the basis of the strength of the 0- 6-km mean wind or other factors the forecaster then could select for analysis the deviation deemed most appropriate for the situation. This output format would also help the forecaster assess whether the risk is widespread or localized. If helicity values are large regardless of deviation, the potential for low-level rotation is more extensive than if helicity values become significant only with extreme right deviation. This or a similar format could be used to generate helicity output maps from sources such as rawinsonde data, profiler and WSR-88D wind data, and numerical model forecasts.

7. Bulk Richardson Number Shear (U) Results

As discussed in section 1, the Bulk Richardson Number (BRN) shear, U [*Weisman and Klemp*, 1982, 1986], is a parameter that measures the ambient environmental shear that is important for supercell development:

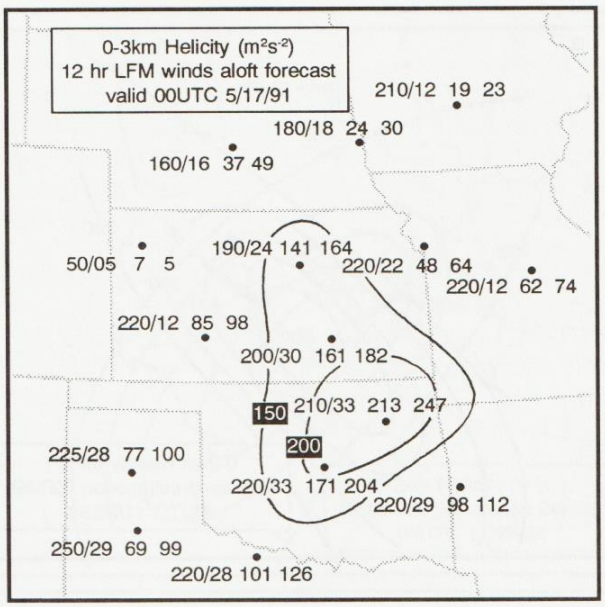

Fig. 1. Example of 12-hour forecast of 0- 3-km AGL integrated storm-relative helicity, derived from LFM forecast winds aloft data and surface data from MOS guidance valid at 0000 UTC May 17, 1991, for sites at approximate dot locations. Three computations are indicated for each site: the first number/group is the 0- 6-km AGL mean wind direction and speed in degrees and knots; the second and third numbers are helicity values derived using storm motions of 20R85 and 30R75 (see text for explanation of annotation), respectively. The 30R75 helicity (third number) is analyzed for values ≥ 150 m^2 s^{-2}. In this particular case the LFM guidance verified reasonably well, and damaging supercell-induced tornadoes occurred near Wichita and Tulsa.

U = the straight vector difference between the 0- 6-km AGL mean wind and the boundary layer wind (i.e., 0- 500-m AGL mean wind)

Units are m s^{-1}. It is important to note that although the BRN correlates reasonably well with observed storm type (e.g., supercell versus multicell), it is a poor predictor of storm rotation in low levels because it does not account for some aspects of the wind profile, such as low-level curvature shear [*Lazarus and Droegemeier*, 1990].

Figure 2 shows the distribution of U for the JDL data set. The majority of cases (70%) are associated with U values greater than 18, with one case exceeding 40. None of the cases has a U value less than 12. This suggests that U values much less than 12 m s^{-1} may not be able to support supercell-induced tornadoes.

8. Middle-Level Wind Speed Results

Doswell [1991] specifies middle-level winds as those in roughly the 700- to 500-mbar layer. For consistency when dealing with surface elevations ranging from the high plains to ocean coastal areas, this study considers the mean measured wind speed in the 3- 6-km AGL layer as representative of middle levels.

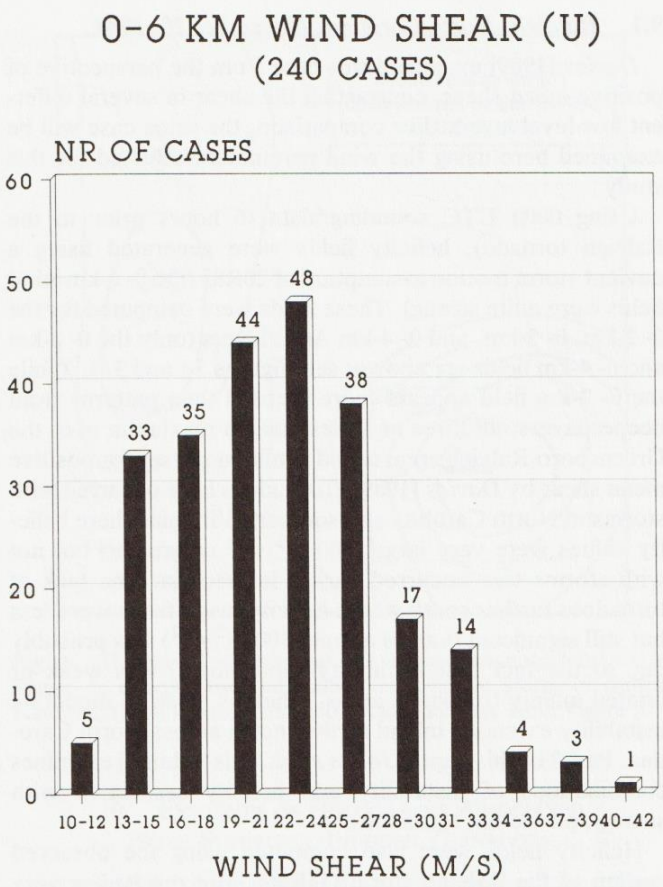

Fig. 2. Distribution of cases from JDL data set, grouped according to U magnitude (Bulk Richardson Number shear) (in units of meters per second).

The average mean 3- 6-km wind speed for the JDL data set is 49 knots (24 m s^{-1}). The average mean 3- 6-km wind speed for relatively weak wind cases (0- 6-km mean wind speed $\leq$30 knots (15 m s^{-1})) is 34 knots (17.5 m s^{-1}). The lowest mean 3- 6-km wind speed encountered in the data set is 20 knots (11 m s^{-1}), which agrees with Doswell's observation that middle-level winds should generally be 20 knots (11 m s^{-1}) or greater regarding hodographs that indicate potential for supercell development.

9. Case Studies

Horizontal fields generated from sounding data for parameters selected for this study will be examined briefly here for two cases from the 31-case storm motion subset, one involving strong wind fields and one involving less intense wind fields. These serve as examples of how wind parameters might come together diagnostically to indicate potential for tornadic supercell development. However, the forecaster needs to remember that atmospheric wind profiles are changing constantly. The reader is referred to *Doswell* [1991] for a discussion concerning the problems of forecasting changes to the hodograph/wind profile.

9.1. *Raleigh, North Carolina, November 28, 1988*

Davies [1989] examined this case from the perspective of positive mean shear, contrasting the shear in several different low-level layers. For comparison, the same case will be examined here using the wind parameters selected for this study.

Using 0000 UTC sounding data (6 hours prior to the Raleigh tornado), helicity fields were generated using a deviant storm motion assumption of 20R85 (the 0- 6-km wind fields were quite strong). These fields were computed for the 0- 2-km, 0- 3-km, and 0- 4-km AGL layers (only the 0- 2-km and 0- 4-km fields are shown; see Figures 3*a* and 3*b*). While the 0- 2-km field appears more focused than patterns from deeper layers, all three analyses place a maximum over the Greensboro-Raleigh area, as did similar analyses for positive mean shear by *Davies* [1989]. Tornadoes later occurred with storms in North Carolina and southern Virginia where helicity values were very large (600 m^2 s^{-2} or greater) but not with storms that occurred earlier in Georgia. The lack of tornadoes further south where helicity magnitudes were less but still significant (values around 300 m^2 s^{-2}) was probably due to the fact that instability (not shown) was weak or limited mainly to coastal areas, whereas weak to moderate instability extended inland further north across North Carolina. Part 2 of this paper [*Johns et al.*, this volume] examines combinations of instability and helicity associated with strong and violent tornadoes.

Helicity fields were also computed using the observed motion of the Raleigh storm (24R86). The results are very similar to the fields derived using an assumed motion. This can be seen by comparing the 0- 2-km fields in Figures 3*a* and 4 (the 0- 3-km and 0- 4-km observed helicity fields are not shown). In this case the use of an assumed storm motion of 20R85 relative to the 0- 6-km mean wind worked quite well in offering a useful diagnostic depiction of the helicity.

Bulk Richardson Number shear U (not shown) was strong with a maximum of more than 28 m s^{-1} over central North Carolina. Middle-level winds (not shown) were also strong, ranging from 40 to more than 80 knots (20–40 m s^{-1}) over the eastern United States. Considering just the wind criteria in this case (apart from other factors such as instability), all parameters are more than adequate for supercell development, most over a large area. It is the helicity pattern that is most helpful in narrowing the threat area, particularly the 0-2-km field. This is typical of tornado cases involving strong wind fields.

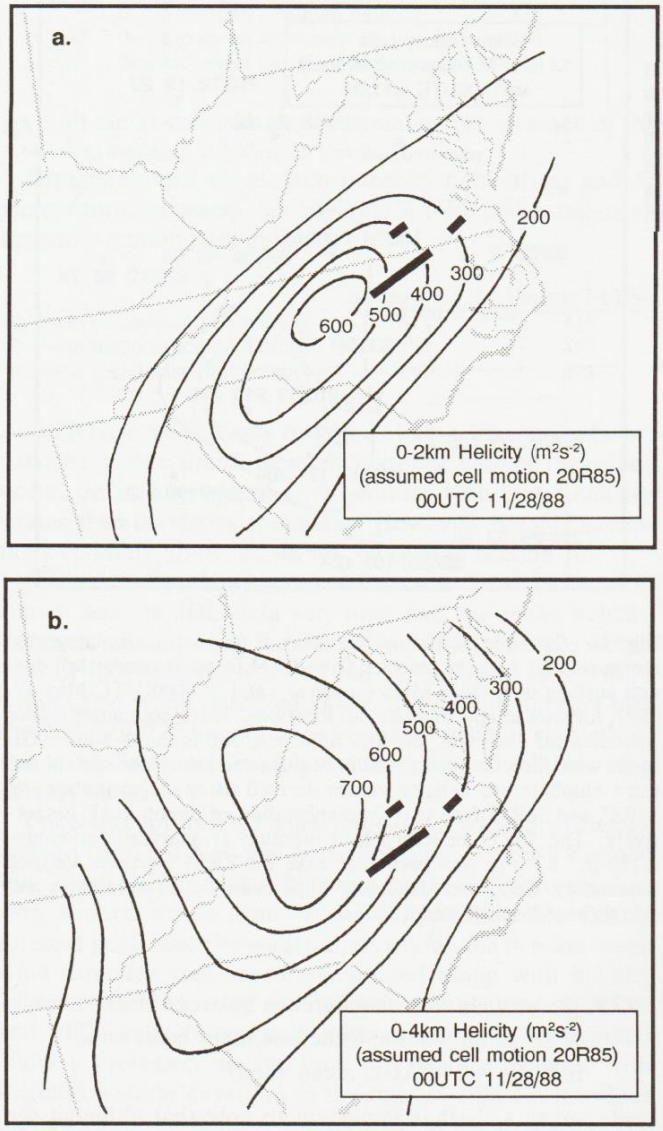

Fig. 3. Horizontal distribution of storm-relative helicity subjectively analyzed from 0000 UTC November 28, 1988, sounding data, using an assumed storm motion of 20R85. Helicity is integrated through (*a*) 0–2 km AGL and (*b*) 0–4 km AGL. Units of contours are m^2 s^{-2}. Heavy lines represent tracks of significant tornadoes which occurred 6–8 hours after 0000 UTC.

9.2. *Central Kansas/Southeast Wyoming, May 24, 1990*

Figure 5 shows the 0- 2-km assumed helicity field (the 0-3-km and 0- 4-km fields are not shown) from 0000 UTC May 25, 1990, sounding data, when significant supercell-induced tornadoes were occurring over central Kansas and southeast Wyoming. The wind fields are weaker than in the Raleigh case (0- 6-km mean wind $\leq$30 knots (15 m s^{-1}) over a majority of the area), so a 30R75 motion assumption was applied. Note that even with the coarse resolution of the rawinsonde network, two general areas of maximum helicity are evident, each roughly corresponding to the locations of tornado occurrences. The assumed helicity depictions compare well with analyses generated using observed storm motions (the observed helicity field for 0–2 km is shown in Figure 6).

An analysis of BRN shear U (Figure 7) indicates two maximum areas/ridges of strong shear through middle levels, one over Kansas and another extending from western Colorado into the northern high plains. Middle-level wind speeds

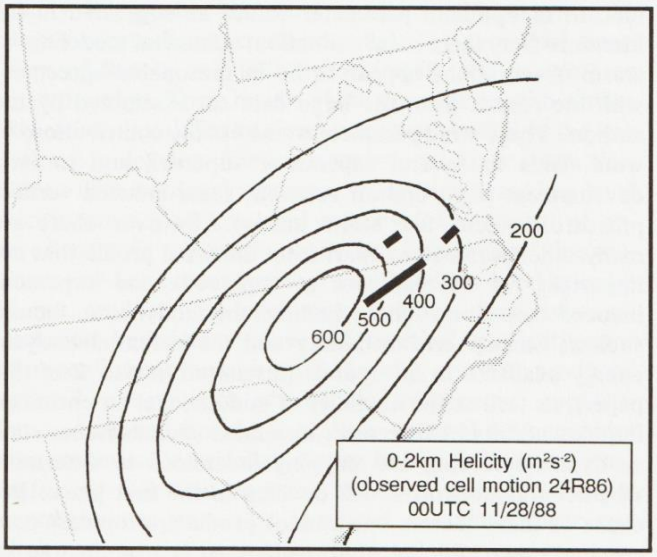

Fig. 4. Horizontal distribution of storm-relative helicity as in Figure 3*a*, except observed motion of Raleigh tornadic storm (24R86) is used. Tornado tracks are as in Figure 3.

(3- 6-km AGL averages) in Figure 8 reveal two streams of maximum winds, each correlating well with the *U* parameter shear maxima in Figure 7. These wind maxima are moving downstream across the areas of tornado occurrence, providing shear through middle levels and additional support for supercell thunderstorms.

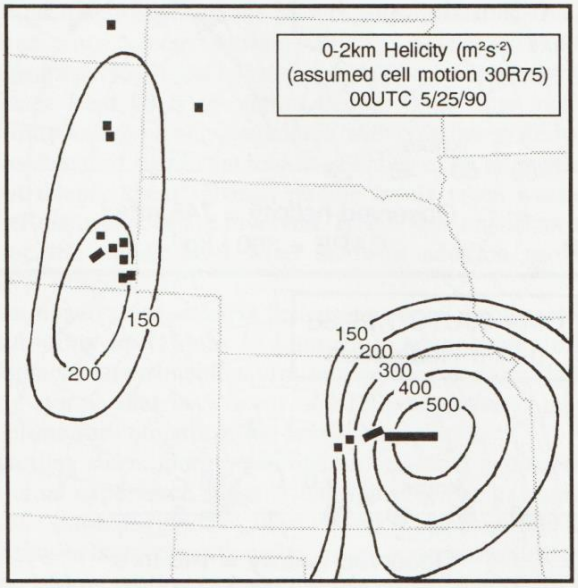

Fig. 5. Horizontal distribution of storm-relative helicity integrated through 0–2 km AGL, subjectively analyzed from 0000 UTC May 25, 1990, rawinsonde network data using an assumed storm motion of 30R75. Units of contours are $m^2 s^{-2}$. Square dots and heavy lines represent approximate locations of tornadoes occurring within 2–3 hours of 0000 UTC.

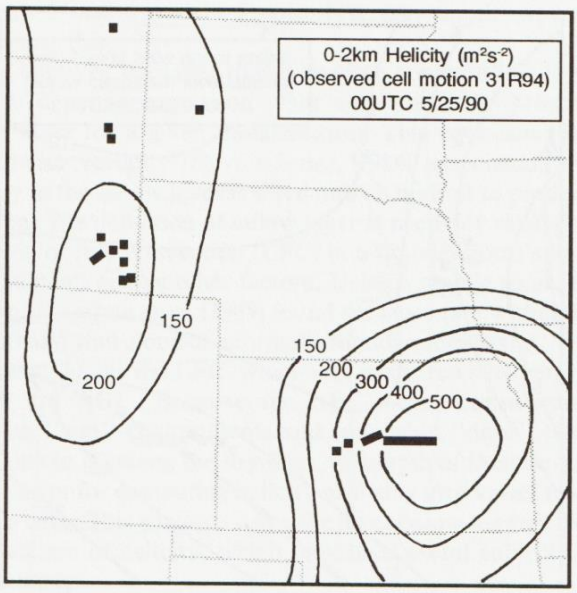

Fig. 6. Horizontal distribution of storm-relative helicity as in Figure 5, except observed motion of tornadic storm in central Kansas (31R94) is used. Tornado occurrences are as in Figure 5.

10. Extremes of Hodographs Associated With Supercell-Induced Tornadoes

Examination of the large JDL data set exposed the authors to a wide range of wind profiles that were associated with strong and violent tornadoes. While many hodographs were

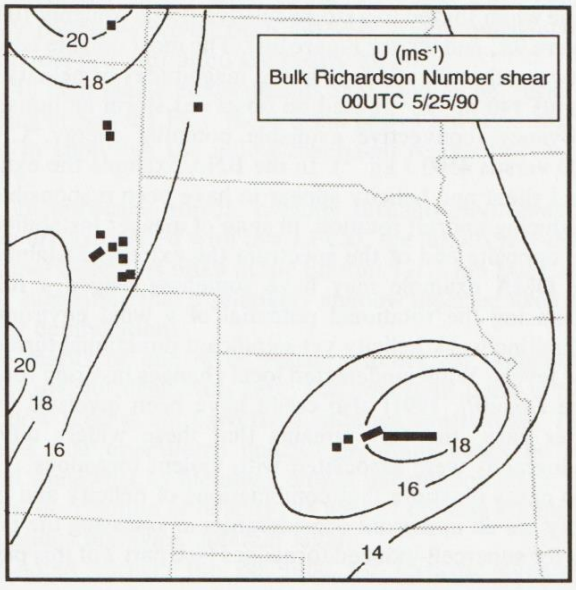

Fig. 7. Horizontal distribution of *U* (Bulk Richardson Number shear) subjectively analyzed from 0000 UTC May 25, 1990, rawinsonde network data. Units of contours are meters per second. Tornado occurrences are as in Figure 5.

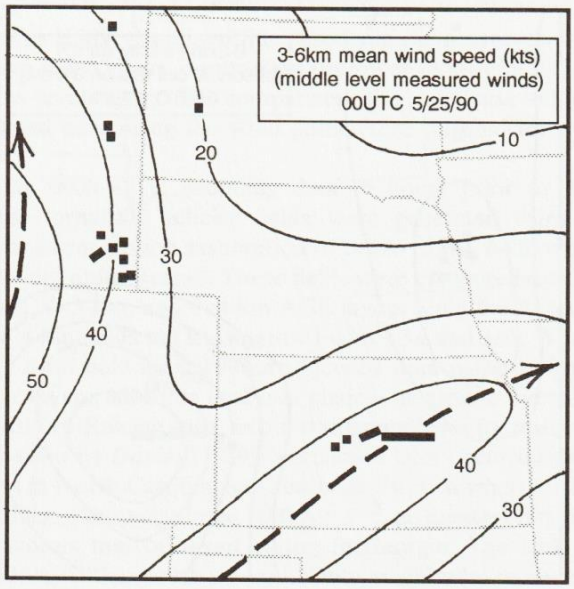

Fig. 8. Horizontal distribution of mean 3- 6-km AGL wind speed subjectively analyzed from 0000 UTC May 25, 1990, rawinsonde network data. Units of contours are knots. Heavy dashed lines are axes of maximum wind speed. Tornado occurrences are as in Figure 5.

similar in scope and shape, the extremes of hodographs encountered are significant and are worth discussing briefly.

Figure 9 shows two low-level hodographs from the JDL data set that are quite different from each other in size and scope. Both hodographs were associated with tornadoes of F4 intensity. While not obvious in a ground-relative frame, the directional turning for both hodographs is nearly the same when shifted to a storm-relative frame (roughly 100° for Figure 9*a*, and 90° for Figure 9*b*). The most notable contrast between the two cases is in the magnitudes of helicity (745 versus 140 $m^2 s^{-2}$, based on observed storm motions) and buoyancy (convective available potential energy, CAPE) (300 versus 4500 J kg^{-1}). In the BNA example the extreme wind shear and helicity appear to have been responsible for producing updraft rotation, in spite of meager instability. At the opposite end of the spectrum the extreme instability in the OMA example may have somehow played a role in enhancing the rotational potential of a wind environment exhibiting weak helicity yet significant directional turning in low levels. While undetected local changes favoring rotation [see *Doswell*, 1991] also could have been involved in the latter case, the fact remains that these widely differing hodographs were associated with violent tornadoes. These two cases illustrate that combinations of helicity and instability are an important consideration in assessing the potential for supercell-induced tornadoes (see part 2 of this paper).

11. Discussion

The wind parameters examined in this study appear to relate well to supercell-induced tornado development. Significant or optimum parameter values as suggested in the literature from theoretical deduction, numerical modeling, or storm observations appear to be in reasonable agreement with the results from the large data set assembled by the authors. These wind parameters address the contributions of wind fields to several aspects of supercell and tornado development (e.g., updraft rotation, shear-induced vertical pressure gradient, and storm inflow). However, there are many other parameters apart from the wind profile that are important for development of supercells and supercell-induced tornadoes. These include thermodynamic factors such as atmospheric instability and the potential buoyant energy available to an updraft (discussed in part 2 of this paper), as well as the humidity of middle-level air entrained into downdrafts. A forecaster also must address issues such as dynamic forcing and capping inversions to determine whether thunderstorms will develop in the first place. Because of these factors one cannot produce a forecast concerning supercell-induced tornadoes from examination of wind parameters alone. However, it does appear that sufficient critical or "optimum" values of the wind parameters must be present for thunderstorms to develop into supercells that produce tornadoes.

While statistical correlations of the selected wind parameters to tornado occurrence and likelihood are beyond the scope of this study, some subjective comments can be offered regarding their relative usefulness in forecasting.

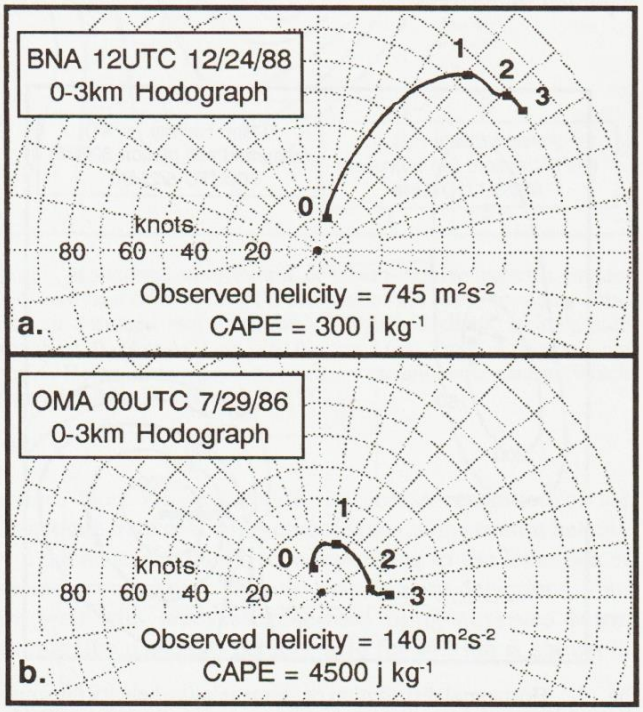

Fig. 9. Ground-relative low-level hodographs (0–3 km AGL) for (*a*) Nashville, 1200 UTC December 24, 1988, and (*b*) Omaha 0000 UTC July 29, 1986. Each ring increment represents 10 knots (5 m s^{-1}).

Helicity is probably the most crucial wind parameter for indicating tornadic supercell potential. The numerical simulations of *Brooks and Wilhelmson* [1990] tend to reinforce this impression. Their results show that storms with similar BRN values but differing shear curvature profiles in the low levels often develop differing circulations. Their storm simulations with low-level curvature shear (significant low-level helicity) developed low-level mesocyclones typical of observed tornadic supercells, while simulations involving rectilinear low-level shear (weak or negligible low-level helicity) did not produce low-level mesocyclones. Both types of simulations had similar values of U (vertical "straight-vector difference" shear through middle levels), and both produced supercell storms with identifiable middle-level mesocyclones. Although *Brooks et al.* [this volume] did encounter some numerically modelled storms in high-helicity environments that failed to produce low-level mesocyclones, it nevertheless appears that low-level curvature shear and helicity are crucial factors for the development of mesocyclones at low levels.

Positive mean shear correlates well with helicity in most cases involving moderate to strong wind fields and is a useful alternate calculation in such situations. As the positive mean shear becomes greater, the inference is that a larger range of storm motions can support tornadic supercell development. However, when wind fields are relatively weak (yet adequate to support supercell development), helicity is the preferable parameter because it can provide a useful depiction of the enhancement of rotational potential due to a storm's local motion.

Because deeper vertical shear (through middle levels) is an important ingredient for supporting supercells, the BRN shear and the strength of the middle-level winds also have importance in a forecast setting. Although most cases exhibiting significant low-level helicity also will be associated with significant wind fields through a deeper layer (due to the baroclinity and dynamics associated with weather systems), it is possible that significant low-level helicity can be present without deeper shear through middle levels when weaker weather disturbances are involved. Hence it is important to examine the middle-level wind fields in addition to the low-level helicity.

Returning to storm-relative helicity as a crucial parameter, key questions are (1) how to estimate in advance of storm development a reasonable storm motion for the more right-moving storms that may occur and (2) what layer is most appropriate for computing low-level helicity.

Regarding storm motion estimation, section 5 and recent operational experience suggest that applying one exclusive "preset" storm deviation in all situations is inappropriate for estimating helicity operationally. From examination of the 31-case storm motion subset the idea that supercells in weaker wind environments tend to deviate more from the mean wind has some validity. Therefore it would seem appropriate for a forecaster to be able to "phase in" larger deviations as wind fields become weaker for purposes of computing helicity. The 20R85/30R75 scheme suggested in sections 5 and 6 and in Figure 1 is one simple way of addressing this.

The depth of the layer that is used to compute low-level helicity depends largely on what constitutes the primary inflow layer for a given thunderstorm. This is because the streamwise vorticity [*Davies-Jones*, 1984] associated with helicity in the inflow layer is tilted into an updraft to produce rotation. The definition of inflow layer is probably related to the level of free convection (LFC) in a thunderstorm's near environment, among other factors. Using a mobile sounding system, *Bluestein et al.* [1989] found the lapse rate within the updraft and wall cloud of a tornadic thunderstorm to be "wet adiabatic" above the LFC, which was measured between 1.5 and 2 km AGL. Because the LFC varies considerably between "wet" environments and somewhat "drier" environments (e.g., along the dry line), the depth of the relevant inflow layer for computing helicity probably also varies from case to case. This suggests using the layer below the LFC for computation of helicity, which may be a useful subject for future study.

Operationally, different studies have used different layers for computing helicity. *Davies-Jones et al.* [1990] use 0-3-km AGL for the general inflow layer, while *Woodall* [1990] computes helicity for a deeper layer (0- 4-km AGL). From this study, the vertical distribution of helicity (section 6) and the case studies (section 9) suggest that useful results can often be obtained using the 0- 2-km AGL layer. On the basis of the examination of data set and recent operational experience the following general comments are offered.

1. Helicity derived from the 0- 2-km layer often tends to focus the horizontal pattern into a more useful area diagnostically (see Figure 3), while helicity patterns from deeper layers tend to spread out. This is particularly true in situations involving strong wind fields. In weak wind fields, helicity patterns derived from different layers (particularly 0–2 km and 0–3 km) often are nearly identical.

2. In high plains environments that tend to be "drier," resulting in higher LFCs, the 0- 3-km or 0- 4-km layer works better in capturing the inflow layer and relevant areas of helicity.

3. In hurricane/tropical cyclone tornado environments (which are associated with low LFCs), the largest low-level shear and helicity is often in the bottom 1–1.5 km [*McCaul*, 1991], suggesting that a relatively shallow layer be used for helicity computation.

The merits of one layer versus another for computing helicity are not dealt with here; the important point is that the inflow layer is not fixed from situation to situation. This suggests that operational helicity programs might be improved somewhat by including output information about the vertical distribution of helicity, as well as offering computation options involving different layers.

As noted earlier, the potential for tornadic supercell development does not depend on wind parameters alone. Part 2 of this paper [*Johns et al.*, this volume] will examine combinations of instability and shear/helicity that are associated with strong and violent supercell-induced tornadoes.

Acknowledgments. The authors wish to thank Grant Bean, Dave Higginbotham, and other NSSFC computer staff in helping to assemble the large data set used for this study. Ken Howard, NSSL, ERL; Mike Ryba, WSO DDC; and Joe Schaefer, SSD, Central Region NWS, are also acknowledged for their help with this project.

References

Bluestein, H. B., and C. R. Parks, A synoptic and photographic climatology of low-precipitation severe thunderstorms in the southern plains, *Mon. Weather Rev., 111*, 2034–2046, 1983.

Bluestein, H. B., E. W. McCaul, Jr., G. P. Byrd, G. R. Woodall, G. Martin, S. Keighton, and L. C. Showell, Mobile sounding observations of a tornadic thunderstorm near the dryline: The Gruver, Texas storm complex of 25 May, 1987, *Mon. Weather Rev., 117*, 244–250, 1989.

Brooks, H. E., and R. B. Wilhelmson, The effects of low-level hodograph curvature on supercell structure, in *Preprints, 16th Conference on Severe Local Storms*, pp. 34–39, American Meteorological Society, Boston, Mass., 1990.

Brooks, H. E., C. A. Doswell III, and R. P. Davies-Jones, Environmental helicity and the maintenance and evolution of low-level mesocyclones, this volume.

Darkow, G. L., and D. W. McCann, Relative environmental winds for 121 tornado bearing storms, in *Preprints, 11th Conference on Severe Local Storms*, pp. 413–417, American Meteorological Society, Boston, Mass., 1977.

Davies, J. M., On the use of shear magnitudes and hodographs in tornado forecasting, in *Preprints, 12th Conference on Weather Forecasting and Analysis*, pp. 219–224, American Meteorological Society, Boston, Mass., 1989.

Davies-Jones, R. P., Streamwise vorticity: The origin of updraft rotation in supercell storms, *J. Atmos. Sci., 41*, 2991–3006, 1984.

Davies-Jones, R. P., D. W. Burgess, and M. Foster, Test of helicity as a tornado forecast parameter, in *Preprints, 16th Conference on Severe Local Storms*, pp. 588–592, American Meteorological Society, Boston, Mass., 1990.

Doswell, C. A., III, A review for forecasters on the application of hodographs to forecasting severe thunderstorms, *Natl. Weather Dig., 16*, 2–16, 1991.

Doswell, C. A., III, A. R. Moller, and R. W. Przybylinski, A unified set of conceptual models for variations on the supercell theme, in *Preprints, 16th Conference on Severe Local Storms*, pp. 40–45, American Meteorological Society, Boston, Mass., 1990.

Johns, R. H., J. M. Davies, and P. W. Leftwich, An examination of the relationship of 0–2 km AGL "positive" wind shear to potential bouyant energy in strong and violent tornado situations, in *Preprints, 16th Conference on Severe Local Storms*, pp. 593–598, American Meteorological Society, Boston, Mass., 1990.

Johns, R. H., J. M. Davies, and P. W. Leftwich, Some wind and instability parameters associated with strong and violent tornadoes, 2, Variations in the combinations of wind and instability parameters, this volume.

Lazurus, S. M., and K. K. Droegemeier, The influence of helicity on the stability and morphology of numerically simulated storms, in *Preprints, 16th Conference on Severe Local Storms*, pp. 269–274, American Meteorological Society, Boston, Mass., 1990.

Lilly, D. K., The structure, energetics, and propagation of rotating convective storms, II, Helicity and storm stabilization, *J. Atmos. Sci., 43*, 126–140, 1986.

Maddox, R. A., An evaluation of tornado proximity wind and stability data, *Mon. Weather Rev., 104*, 133–142, 1976.

McCaul, E. W., Jr., Simulations of convective storms in hurricane environments, in *Preprints, 16th Conference on Severe Local Storms*, pp. 334–339, American Meteorological Society, Boston, Mass., 1990.

McCaul, E. W., Jr., Buoyancy and shear characteristics of hurricane-tornado environments, *Mon. Weather Rev., 119*, 1954–1978, 1991.

Rasmussen, E. N., and R. B. Wilhelmson, Relationships between storm characteristics and 1200 GMT hodographs, low-level shear, and stability, in *Preprints, 13th Conference on Severe Local Storms*, pp. J5–J8, American Meteorological Society, Boston, Mass., 1983.

Rotunno, R., and J. B. Klemp, The influence of the shear-induced vertical pressure gradient on thunderstorm motion, *Mon. Weather Rev., 110*, 136–151, 1982.

Wakimoto, R. M., and J. W. Wilson, Non-supercell tornadoes, *Mon. Weather Rev., 117*, 1113–1140, 1989.

Weisman, M. L., and J. B. Klemp, The dependence of numerically simulated convective storms on vertical wind shear and buoyancy, *Mon. Weather Rev., 110*, 504–520, 1982.

Weisman, M. L., and J. B. Klemp, Characteristics of isolated convective storms, in *Mesoscale Meteorology and Forecasting*, edited by P. S. Ray, pp. 331–358, American Meteorological Society, Boston, Mass., 1986.

Woodall, G. R., Qualitative forecasting of tornadic activity using storm-relative environmental helicity, in *Preprints, 16th Conference on Severe Local Storms*, pp. 311–315, American Meteorological Society, Boston, Mass., 1990.